Paper # 108

Effect of the crosslink density and sulfur-length on wet-traction and rolling resistance performance indicators for passenger car tire tread materials

Ernest Cichomski[1], Wilma K. Dierkes[1],

Jacques W.M. Noordermeer[1], Steven M. Schultz[2], Tanya V. Tolpekina[2], Louis A.E.M. Reuvekamp[1, 2], Anke Blume[1*]

[1]Department of Elastomer Technology and Engineering, University of Twente, P.O.Box 217, 7500AE Enschede, the Netherlands

[2]Apollo Tyres Global R&D B.V., P.O. Box 3795, 7500 DT | Colosseum 2, 7521 PT Enschede, the Netherlands

Presented at the Fall 188th Technical Meeting of
Rubber Division, ACS
Cleveland, OH
October 13-15, 2015

ISSN: 1547-1977

* Speaker

ABSTRACT

The scope of this study is the investigation of the influence of different sulfur vulcanization systems for silica reinforced SBR/BR blends on the performance indicators of tire treads made thereof. Three series of compounds were prepared: with conventional, semi-efficient and efficient vulcanization systems. Each vulcanization system results in a specific overall crosslink density and different sulfur rank distribution: mono-, di- and polysulfidic of nature. The experimental results indicate that the influence of the overall crosslink density on the value of tan δ at 60 °C, an indication of rolling resistance, is higher than the type of crosslinks: A higher density of crosslinks reduces energy losses by limiting the segmental mobility of the polymer chains. Differences between the vulcanization systems manifest themselves only at relatively high strain levels, exceeding those used during measurements of the tan δ values at 60 °C. The dynamic mechanical analysis shows an increase in the glass transition temperature with rising overall crosslink densities. The influence of different crosslink densities on the LAT100 side force coefficient values, which are an indication of wet skid resistance of tire treads, is discussed in detail.

INTRODUCTION

Beside the elastomer type and silica-silane system, the crosslink density and distribution are important parameters which affect the physical, mechanical and viscoelastic properties of a vulcanizate [1,2,3]. Sulfur and organic peroxides are the two most commonly used vulcanizing agents. Unlike in a peroxide-cured system, in accelerated sulfur-curing systems various complex reactions occur during the curing process that form either mono-, di-, or polysulfidic crosslinks, and sulfidic ring structures within the polymer chains [4,5]. The ratio of accelerator to crosslinking

agent determines the type and density of the crosslinks [6,7]. An accelerator increases the rate of cure and the efficiency with which sulfur is used in crosslinking compared to further possible side reactions. The concentration of sulfidic linkages between carbon atoms of the polymer chains can be adjusted by varying the amounts of sulfur and accelerator [8]. High sulfur levels, e.g. 2 to 3.5 phr, and low levels of accelerator, 0.5 to 1 phr, generally described as conventional vulcanizing systems (CV), result in mostly highly flexible polysulfidic networks ([-C-S_x-C-] where $x \geq 2$) with good mechanical properties [9,10,11]. However, the aging resistance is poor due to the temperature susceptibility of polysulfidic linkages. In conventional vulcanizations, part of the sulfur modifies the polymer chains instead of crosslink formation. Low sulfur levels, 0.25 to 0.7 phr, with high accelerator levels, 2.5 to 5 phr, commonly known as efficient vulcanizing systems (EV), introduce mono- or disulfidic networks ([-C-S_x-C-] where x = 1 to 2), which exhibit low stress relaxation and good resistance to aging. The third system called semi-efficient vulcanization (SE) with intermediate sulfur and accelerator loadings was introduced to eliminate poor cut growth of the compounds based on natural rubber in which efficient vulcanization was used.

Scheele [12], Saville and Watson [13] and several authors from the Tun Abdul Razak Research Centre (TARRC) [14,15] discussed the network characterization in detail. The work of Ferry et al.[16] described the influence of the crosslink density on the dynamic properties of Natural Rubber (NR). They recognized that the influence of the crosslinking density on the tan δ values in the rubbery zone is significant, whereas in the transition zone it is minor. Hamed and Rattanasom [17,18] highlighted that a higher crosslink density increases the crack propagation and worsens cut growth. Bielinski and Stępkowska [19,20] discussed the tribological properties of carbon black reinforced Emulsion-Styrene-Butadiene Rubber (E-SBR) and showed that an increasing fraction of polysulfidic crosslinks has a minor influence on the friction coefficient. Ramier et al.[21]

investigated the adsorption of accelerators onto the silica surface by the use of different grafting and coupling agents. They concluded that without the grafting agents, the vulcanization seems to be more heterogeneous due to the adsorption of accelerators on the silica surface: crosslinks are more numerous and the polysulfidic bonds are shorter in the filler neighborhood. Greensmith et al.[22] related tensile strength with the crosslink density, and observed that the tensile strength passes through a maximum value with increasing crosslink density. They also reported that the tensile strength of a NR gum decreased in the sequence accelerated sulfur > sulfurless > peroxide > high energy radiation. This observation permitted Mullins [23] to conclude that the tensile strength depends on the type of crosslinks, decreasing in the order polysulphidic > di- and monosulfidic > carbon-carbon, in inverse order of the bonding strength. The general dependence of different mechanical properties on the crosslink density is shown in Figure 1. Despite numerous publications in the field of curing systems, the knowledge concerning the influence of the vulcanization system on tire performance indicators in silica filled synthetic rubber is still limited.

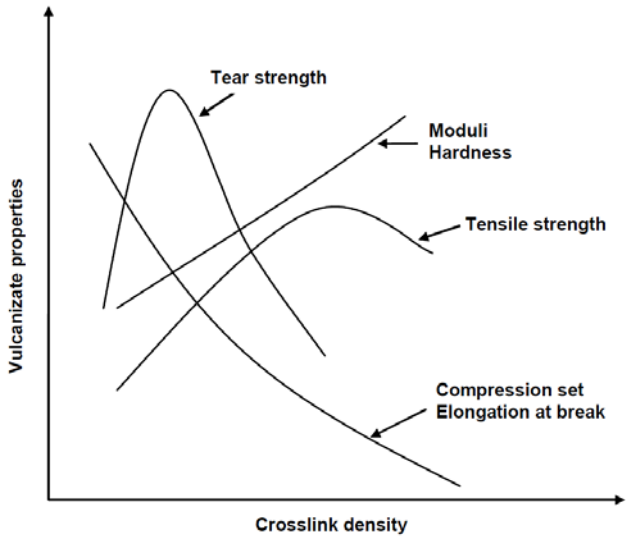

Figure 1: Vulcanizate properties versus crosslink density [24].

EXPERIMENTAL

COMPOUND FORMULATIONS AND MIXING

In order to assess the influence of crosslink density and distribution on tire performance indicators, a series of batches corresponding to conventional, semi-efficient and efficient vulcanization systems were prepared. The ratio of elemental sulfur to N-tert-butyl-2-benzothiazolesulfenamide (TBBS) and diphenylguanidine (DPG) was adjusted to obtain different curing systems, but in order to limit the number of variables the ratio of TBBS to DPG was kept constant. To guarantee the same silica coverage in all the batches, the amount of silane coupling agent was also kept constant. A typical "Green tire" recipe was modified with the desired curing system. Additionally, a reference compound was prepared. Detailed specifications of the ingredients and the formulations are given in Table 1 and 2.

Table 1: Ingredients specification.

Ingredient	Specification	Supplier
S-SBR	Solution Styrene-Butadiene Rubber Buna VSL 5025-2 HM	Lanxess, Germany
BR	High -cis Butadiene Rubber Europrene BR40	Eni Polimeri, Ravenna, Italy
Zeosil 1165	Highly dispersible Silica, BET 160 m^2/g	Solvay, France
TESPT	Bis-(triethoxysilylpropyl)tetrasulfide	Evonik, Germany
TDAE	Treated Distillate Aromatic Extract oil, VivaTec 500	Hansen & Rosenthal, Hamburg, Germany
Zinc oxide	Inorganic oxide	Sigma Aldrich, United States
Stearic acid	Organic acid	Sigma Aldrich, United States
6PPD	Antiozonant N-phenyl-N'-1,3-dimethylbutyl-p-phenylenediamine	Flexsys, Brussels, Belgium
TMQ	Antioxidant 2,2,4- trimethyl-l,2-di-hydroquinoline	Flexsys, Brussels, Belgium
Sulfur	Elemental sulfur, purified by sublimation	Sigma Aldrich, St. Louis, United States
TBBS	Accelerator N-tert-butylbenzothiazole-2-sulphenamide	Flexsys, Brussels, Belgium
DPG	Accelerator - diphenyl guanidine	Flexsys Brussels, Belgium

Table 2: Rubber compound formulations.

Ingredient	Sample code												
	CV-2	**CV-2.5**	**CV-3**	**CV-3.5**	**SE-0.7**	**SE-1.1**	**SE-1.6**	**SE-2**	**EV-0.3**	**EV-0.4**	**EV-0.6**	**EV-0.7**	**Ref.**
SSBR*	103	103	103	103	103	103	103	103	103	103	103	103	103
BR	25	25	25	25	25	25	25	25	25	25	25	25	25
Zeosil 1165 MP	80	80	80	80	80	80	80	80	80	80	80	80	80
TESPT	7	7	7	7	7	7	7	7	7	7	7	7	7
TDAE	5	5	5	5	5	5	5	5	5	5	5	5	5
Zinc oxide	2,5	2,5	2,5	2,5	2,5	2,5	2,5	2,5	2,5	2,5	2,5	2,5	2,5
Stearic acid	2,5	2,5	2,5	2,5	2,5	2,5	2,5	2,5	2,5	2,5	2,5	2,5	2,5
6PPD	2	2	2	2	2	2	2	2	2	2	2	2	2
TMQ	2	2	2	2	2	2	2	2	2	2	2	2	2
Sulfur	**2**	**2,5**	**3**	**3,5**	**0,7**	**1,13**	**1,56**	**2**	**0,25**	**0,4**	**0,55**	**0,7**	**1,4**
TBBS	**0,23**	**0,3**	**0,38**	**0,46**	**0,46**	**0,69**	**0,92**	**1,15**	**1,15**	**1,53**	**1,91**	**2,3**	**1,7**
DPG	**0,27**	**0,36**	**0,44**	**0,54**	**0,54**	**0,81**	**1,08**	**1,35**	**1,35**	**1,8**	**2,25**	**2,7**	**2**

* including 37,5 phr of extender oil

A 1,6 liter Banbury mixer was used for mixing. This process was done in three steps according to the parameters as given in Table 3. The first two steps of the mixing process were done in the internal mixer with an initial set temperature of 40 °C. The dump temperature of the compound was adjusted to be 155 °C by manually changing the cooling water flow and changing the rotor speed, if necessary. Data acquisition was done automatically. Addition of curatives was done on a two roll mill preheated to 50 °C.

Table 3: Mixing procedure.

Stage I	
Rotor speed: 75 RPM Initial temp.: 40 °C	
Timing	Ingredient
(Min. sec.)	
0,0	Add polymers
1,0	Add ½ silica, ½ silane, ZnO + stearic acid
3,0	Add ½ silica, ½ silane, oil, TMQ, 6PPD
4,0	Sweep
6,3	Dump @ ~ 155 °C
Stage II	
Rotor speed: 90 RPM Initial temp.: 40 °C	
Timing	Ingredient
(Min. sec.)	
0,0	Add I stage batch
6,30	Dump @ ~ 155 °C
Stage III	
Mixing in the curatives was performed on a two roll mill	

Vulcanization of the sheeted samples for tensile tests was performed on a Wickert laboratory press (WLP 1600) at 160 °C and 100 bar for an optimal curing time (t_{95}) obtained from Moving Die Rheometer (MDR 2000, Alpha Technologies) measurements according to ISO 6502. The samples for hardness tests were prepared in cylindrical molds and cured for a period of two times t_{90}. The samples for the DIN abrasion test were cured for t_{90} multiplied by 1,2. The adjustment of the curing time as measured in the rheometer was necessary due to the high thickness of the samples and the low thermal conductivity of the rubber compounds.

Characterization methods

The overall apparent crosslink densities and distributions were measured by swelling experiments done in toluene according to Schotman and Datta, Ellis and Moore [25,26,27]. The test sheets were

cut to obtain appropriate test pieces. Propanethiol in combination with piperidine was used to characterize the polysulfidic crosslinks according to the so-called chemical probe method as developed for NR. The further chemical probe method with hexanethiol and piperidine to characterize the poly- plus di- sulfidic crosslinks was carried out as well. Each determination was carried out twice. Because the methods pertain to NR and were never re-worked for SSBR and additionally have never been adapted to silica-reinforced compounds, only the overall apparent crosslink densities and polysulfidic fraction thereof are taken into account.

The Mooney viscosity ML(1+4) of the compounds was measured at 100 °C on a Mooney viscometer MV2000E (Alpha Technologies) according to ISO 289-1. Payne effect measurements were done by using a Moving Die Rheometer, MDR 2000 from Alpha Technologies, after prior vulcanization for 1,2 x t_{90} at 160 °C in the MDR 2000. In order to assess the Payne effect values, the storage modulus at 1% strain and 90% strain were measured at 100°C and a frequency of 0,5 Hz.

Mechanical properties of the samples were tested using a Zwick Z020 tensile tester according to ISO-37. A crosshead speed of 500 mm/min was used. The measurements were done at ambient temperature. Shore A hardness of the samples was measured at five different places on the samples, which were cylindrical with a diameter of 10 mm. The median value is given as a representative hardness of a particular sample.

Abrasion resistance was measured by a DIN abrader machine (Abrasion tester 564C from Karl Frank GmbH) according to method A of DIN 53516. The weight loss was measured and recalculated to a volume loss for each sample.

In order to characterize the wet skid resistance, dynamic mechanical analysis was performed on a Gabo Dynamic Mechanical Analyzer in a temperature-sweep mode from -100 °C to +100 °C with 1 % static and 0,1 % dynamic strain and a frequency of 10 Hz. In order to predict rolling resistance, single point measurements of tan δ = G”/G’, where G’ is the storage modulus and G” is the loss modulus, at 60 °C with 2 % strain and a frequency of 10 Hz were performed.

A Laboratory Abrasion Tester 100 (LAT 100, VMI the Netherlands) was used to estimate the wet skid resistance of the tire treads in conditions which simulate the real conditions on a road[29]: Fig. 1. Wheel samples were made by compression molding in a special mold using the Wickert laboratory vulcanization press for 11 mins. at 170 °C. Testing was performed at five different water temperatures: 2 °C, 8 °C, 15 °C, 22 °C, 30 °C and at constant slip angle of 15°. An electro-corundum disc with relative roughness 180 was used to simulate the tire-road interactions. Tests were performed at constant speed of 1,5 km/h and load of 75 N for a distance of 33 meters. The Side Force Coefficient (SFC) values (Equation 1) for the particular samples are compared with the value obtained for the reference sample and given as relative values. The property with higher rating is always better.

$$SFC = \frac{F_y}{F_z} \qquad \text{(Equation 1)}$$

Where F_y = the side force; and F_z = the normal load on the rubber wheel sample.

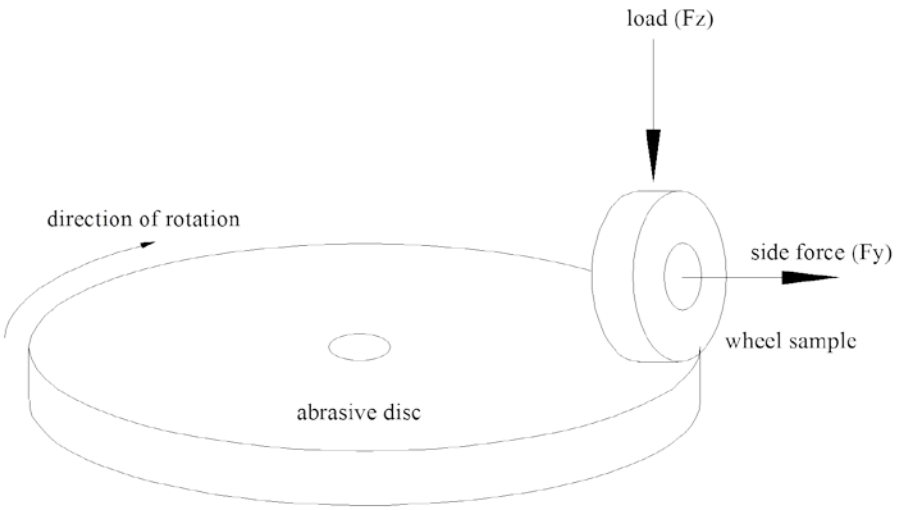

Figure 1: Principle of measurement on the LAT 100.

RESULTS AND DISCUSSION

Crosslink density and sulfur length distribution

The variable ratio of elemental sulfur to accelerators results in different overall crosslink densities and ratios of polysulfidic crosslinks, see Table 4. When lowering the content of elemental sulfur and increasing the amount of accelerators in the compound, the overall crosslink density values decrease. There is a trend away from polysulfidic crosslinks to relatively higher di- and mono-sulfidic ranks.

Table 4: Crosslink densities.

Crosslink density (10^{-4} mol/g)		
Sample code	**Overall**	**Polysulfidic**
CV-2	1,50	0,80 50%
CV-2.5	1,78	1,08 61%
CV-3	1,97	1,11 56%
CV-3.5	2,40	1,54 64%
SE-0.7	0,74	0,29 29%
SE-1.1	1,12	0,57 51%
SE-1.6	1,51	0,81 54%
SE-2	2,04	1,14 56%
EV-0.3	0,74	0,30 41%
EV-0.4	0,97	0,35 36%
EV-0.6	1,31	0,65 50%
EV-0.7	1,63	0,66 40%
Ref.	1,64	0,95 58%

It must be clearly stated that unlike for carbon black reinforced and crosslinked elastomers, each silica particle can be treated as a poly-functional crosslink or nod: The silica surface is chemically bound to polymer chains via the coupling agents. The present measurement of the crosslink density and distribution does not differentiate between the polymer-polymer crosslinks and silica-polymer bonds. Considering that the same loading of TESPT was used in all batches, it is assumed that the amount of silica-polymer bonds also remains relatively unaffected. Hence, these effects may be considered as caused by changes in the density or distribution of the sulfidic crosslinks between the polymer chains.

Mechanical properties

Depending on the overall crosslink density, the highest values of tensile strength are observed for the efficient and semi-efficient crosslinking systems, see Figure 2. For the conventional system, an optimum in tensile strength is barely visible. Additionally, the efficient vulcanization system is also characterized by the highest values of tensile strength in comparison with the two other systems. This behavior is not a commonly observed feature. Two factors needs to be considered in the case of tensile strength: the bond energy of the sulfidic crosslinks and the tendency to crack propagation. A higher bond energy of the mono- and disulfidic crosslinks is responsible for the highest values of the tensile strength for the samples with the efficient curing system. Beside the bond energy, the tendency for a crack propagation is the main cause of low tensile strength values samples with the conventional system: Crack propagation should be easier in compounds with a higher overall crosslink density [17,18]. Hence the samples with conventional vulcanization have the lowest values of the tensile strength.

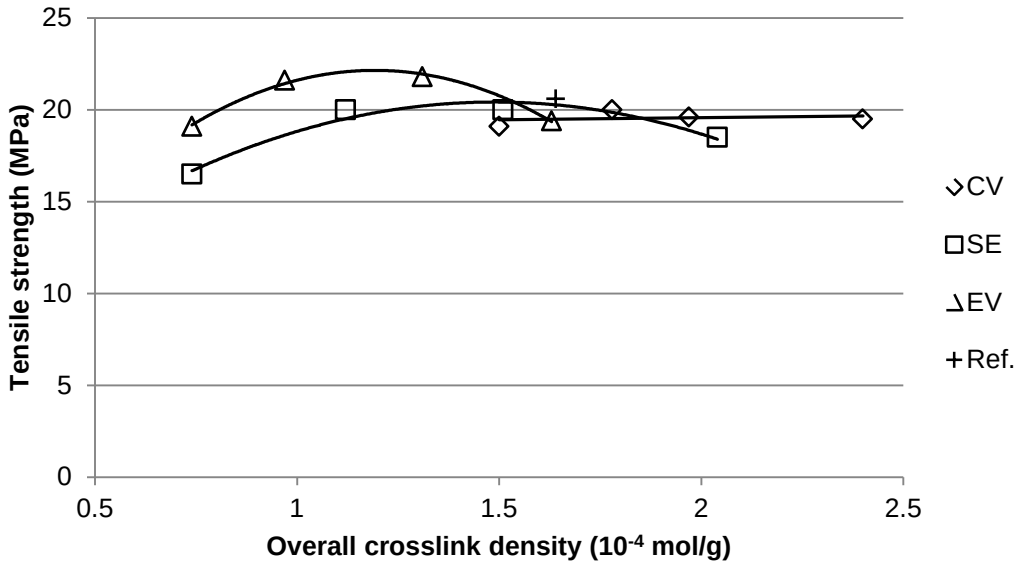

Figure 2: Tensile strength of the compounds with different curing systems.

The higher overall crosslink density is the dominating factor for strength properties, stronger than the well-known ability of the long, poly-sulfidic crosslinks to reformation followed by stress dissipation and increased tensile strength. The semi-efficient system with moderate values of the overall crosslink density ranks somewhere in between the other two curing systems concerning tensile strength.

The initial increase in tensile strength observed for the semi efficient and the efficient vulcanization system can be caused by a primary gain in toughness caused by rising crosslink density. Further increase in crosslink density only increases the stiffness with the risk of getting more brittle material. Compounds with a higher stiffness are more prone to crack propagation what reduces the tensile strength. Furthermore, the appearance of the maximum in tensile strength is not necessarily related to the filler-polymer interaction as other authors reported the appearance of the optimum in the tensile strength also in unreinforced compounds [28].

With increasing overall crosslink density, the values of elongation at break are decreasing for all the crosslinking systems, see Figure 3: The vulcanizates become less elastic what contributes to easier crack formation and sooner breakage of the sample. The conventional system leads to the highest elongation at break values by comparing samples with the same crosslink density. One explanation for this can be that the polysulfidic crosslinks are more able to break and partial reunite again. Another explanation can be that there a higher possibility of movement of the polymer chains having polysulfidic bridges.

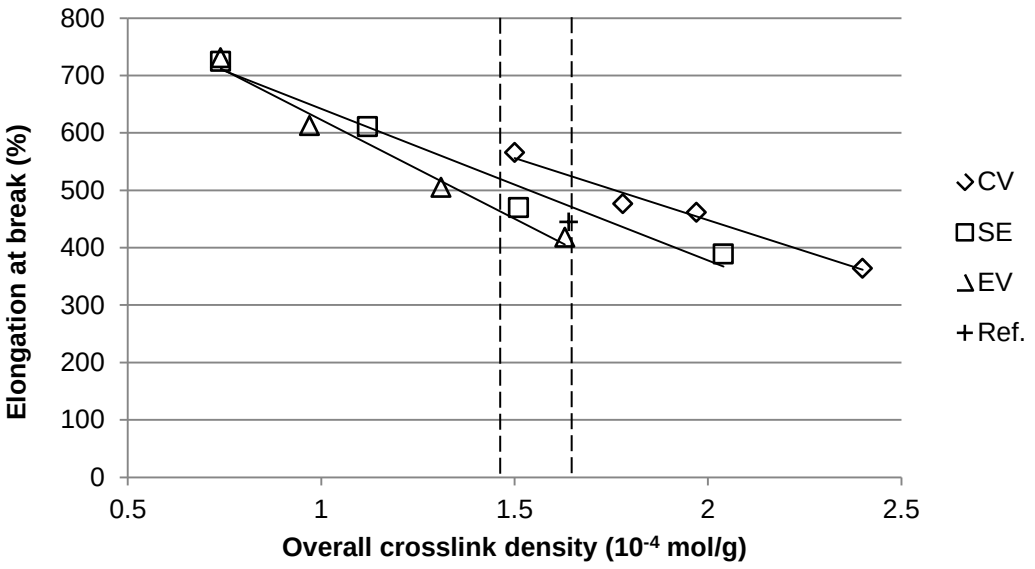

Figure 3: Elongation at break of the compounds with different curing systems.

Abrasion resistance

The EV-vulcanizate with the highest crosslink density is also characterized by the lowest value of abrasion loss in comparison with the semi-efficient and conventional vulcanization systems, see Figure 4. This trend is the same for the SE-material: Increasing the ratio of mono- and disulfidic crosslinks to polysulfidic ones creates a stronger and more durable rubber compound. As a result, a higher force is necessary to cut micro-particles out of the compound by the abrasive micro-asperities.

Additionally, the abrasion loss reaches a minimal value for the SE- and EV-curing system with the highest crosslink density. The EV-curing system is characterized by the highest dependence of abrasion loss on the overall crosslink density. An overall crosslink density higher than $1{,}5 \cdot 10^{-4}$ mol/g seems to lead to a constant abrasion loss.

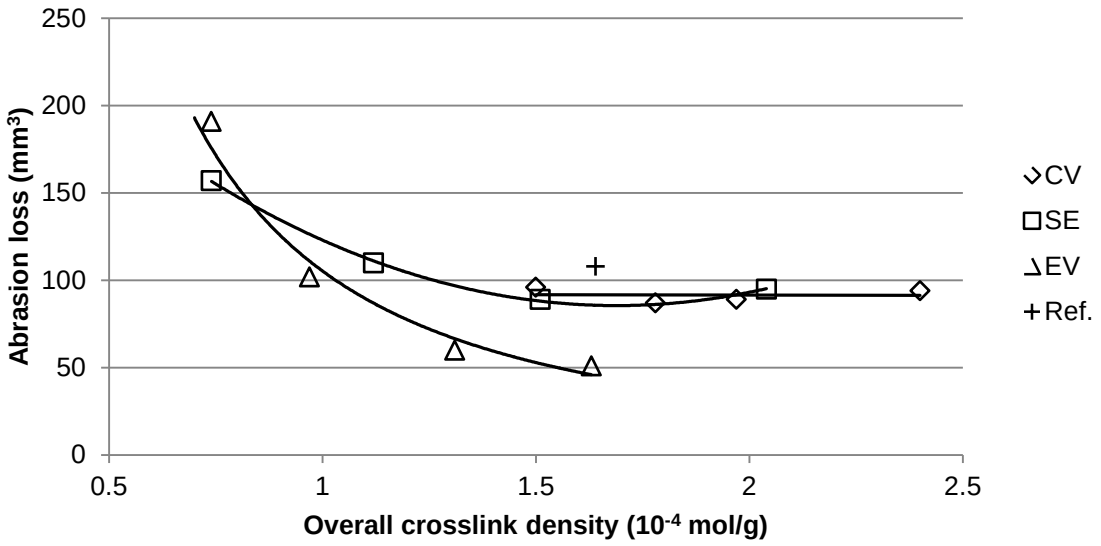

Figure 4: DIN abrasion of the compounds with different curing systems.

Payne effect

In the unvulcanized state, compounds with different curing systems are characterized by mutually comparable values of the storage modulus over the entire range of strains, see Figure 5. In the unvulcanized state, the polymer crosslinks and filler-polymer bonds are not formed yet, therefore they do not contribute to the Payne effect value. Moreover, the comparable values of the storage modulus shown in Figure 5 indicate that in all the cases the silica surface was covered by TESPT and accelerators in a similar manner. Even in the case in which 2,3 phr of TBBS and 2,7 phr of DPG were used ("EV-0.7"), the difference to the system with the lowest accelerator content ("SE-0.7") in the storage modulus is not more than 0,05 MPa. This small difference is caused by the additional adsorption of accelerators on the silica surface. Therefore, the filler-filler interaction are assumed to be similar in all cases, knowing well, that this is not fully correct.

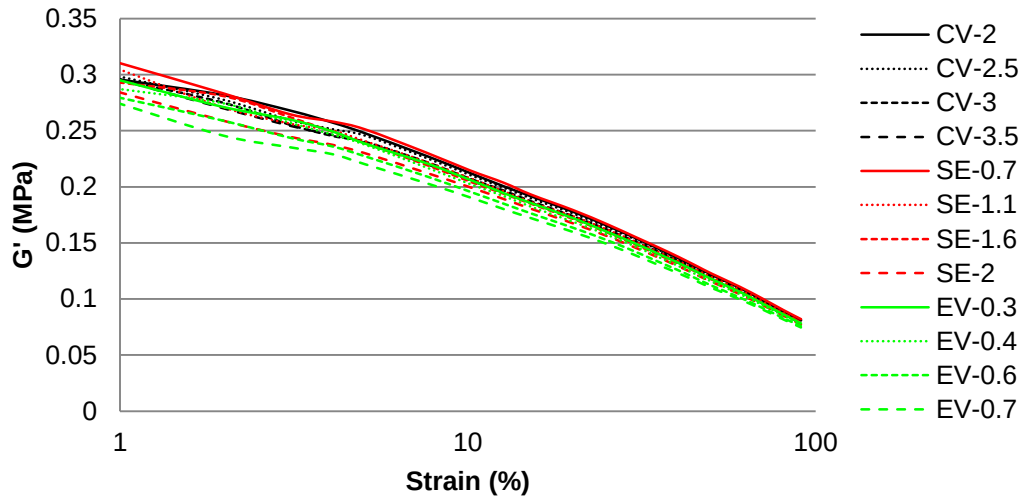

Figure 5: Payne effect versus strain of green compounds.

The vulcanized samples show clear differences in the storage moduli, see Figure 6. The values of the storage modulus at both, very high and very low strain levels, increase with the curative concentrations for each curing system.

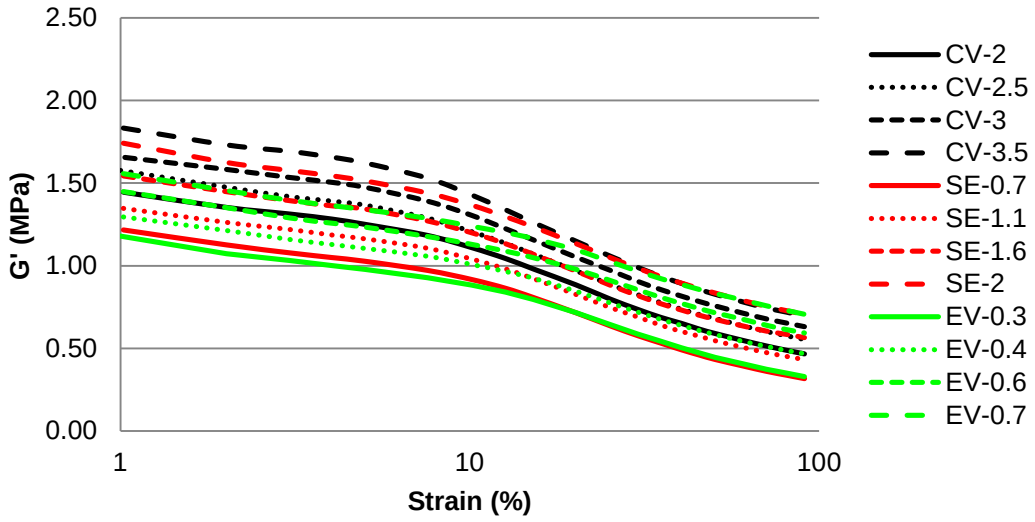

Figure 6: Storage modulus versus strain of cured compounds.

The polymer network, resp. the filler-filler and filler-polymer interactions contribute to the final values of the Payne effect. At low strain level, the deformation energy is mainly stored in the filler network. This network is unstable and gradually disintegrates with increasing strain levels. At the highest strain level the polymer-filler and the remaining undestroyed polymer network are responsible for the energy storage. When the same types and amounts of filler and coupling agent are used, the differences in the filler-filler interaction can be considered as invariable. In general, the energy can be stored more efficiently in a compound with a higher overall crosslink density, because this increases the storage modulus values at both the low and high range of the strain scale.

Comparison between the values of the storage moduli of a compound before and after vulcanization is an example of how the energy storage increases by introduction of the sulfur crosslinks without changes in the filler-filler interactions. The Payne effect can be used to assess the filler-filler interactions only when the crosslink densities and the polymer-filler interactions are similar.

The dependence of the Payne effect on the overall crosslinking density varies for each curing system, see Figure 7. This dependence is stronger for the conventional and semi-efficient systems and fades away for the efficient curing. With increasing content of the polysulfidic crosslinks the Payne effect becomes higher.

The conventional curing system is characterized by the highest Payne effect because of its high storage modulus at low strains which is the result of the highest overall crosslink density. The efficient curing system is characterized by the lowest values of the Payne effect because lower overall crosslink density leads to low values of the storage modulus at low strains. Furthermore, probably the higher percentage of mono- and di-sulfidic crosslinks can last unbroken, preventing

the drop in the value of the storage modulus at high strains. This effect is particularly clear when the samples with the highest concentration of curatives are compared, see Figure 6.

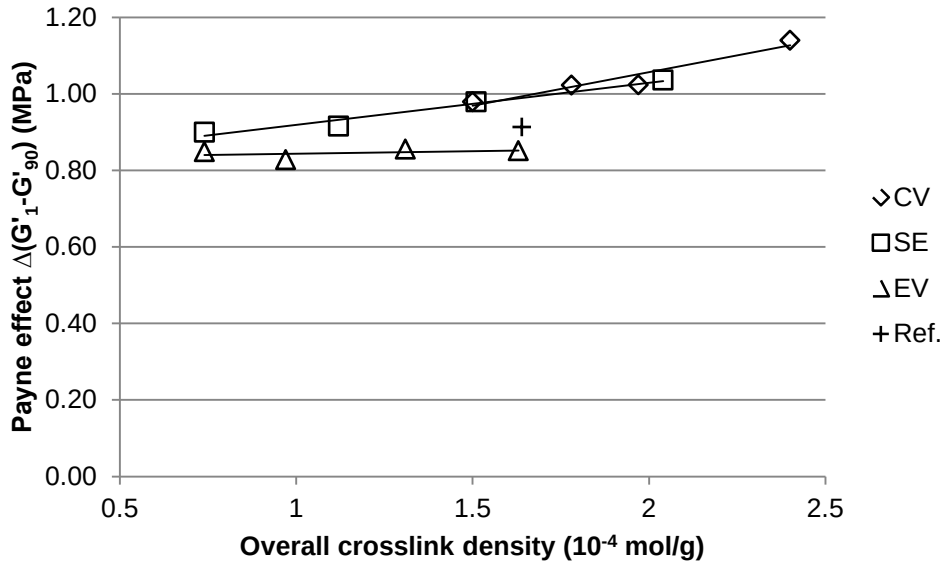

Figure 7. Payne effect of cured samples versus overall crosslink density.

The compounds with the efficient vulcanization system reach higher storage moduli at 90 % strain in comparison with the semi efficient and conventional systems at similar overall crosslink densities, see Figure 8. The higher values of the storage modulus might be the result of differences in the ratios of mono- and disulfidic crosslinks to polysulfidic ones. Apparently, at similar overall crosslink density, a higher percentage of the rigid mono- and disulfidic crosslinks increases the efficiency of energy storage of the compound, which is evident in the higher storage modulus. A higher percentage of polysulfidic crosslinks which are prone to break and recombine more easily during the deformation may be the cause of the lower energy storage capabilities of the CV-compounds.

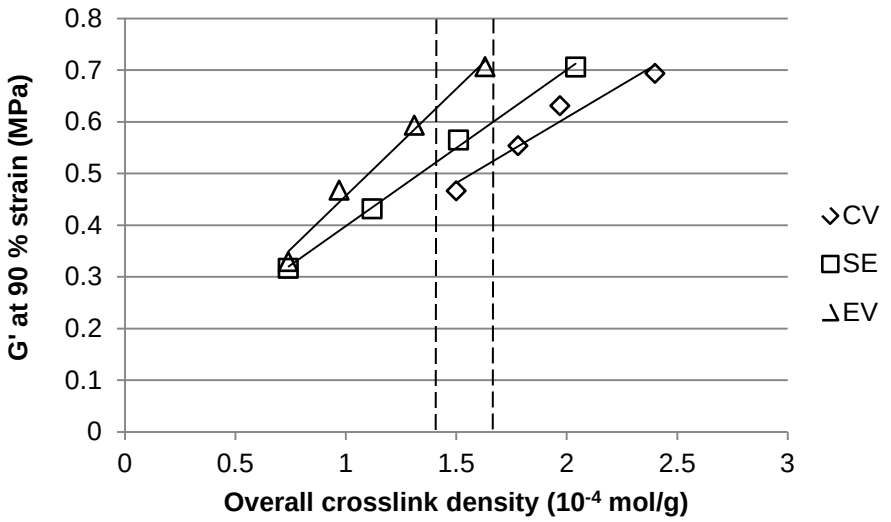

Figure 8: Storage modulus at 90 % strain versus overall crosslink density.

Tan δ at 60 °C: indicator of rolling resistance

Three factors contribute to energy dissipation at higher temperatures: polymer crosslinks, filler-filler and filler-polymer interactions. In this study, the two last factors are considered as quasi constant because all compounds contain the same amount of coupling agent. With this assumption, the differences in the tan δ values at 60 °C are discussed only with the regard to changes in the polymer-polymer crosslinks. The hysteresis of all compounds at 60 °C depends mainly on the overall crosslink density: Figure 9 shows a single correlation for all investigated systems. Therefore, the CV-crosslinked compounds are characterized by the lowest values of tan δ at 60 °C amongst the investigated vulcanization systems due to the highest overall crosslink density. The distribution and type of crosslinks can be considered as negligible for the tan δ values at 60 °C. Patterns as visible in Figure 8 do not appear in Figure 9.

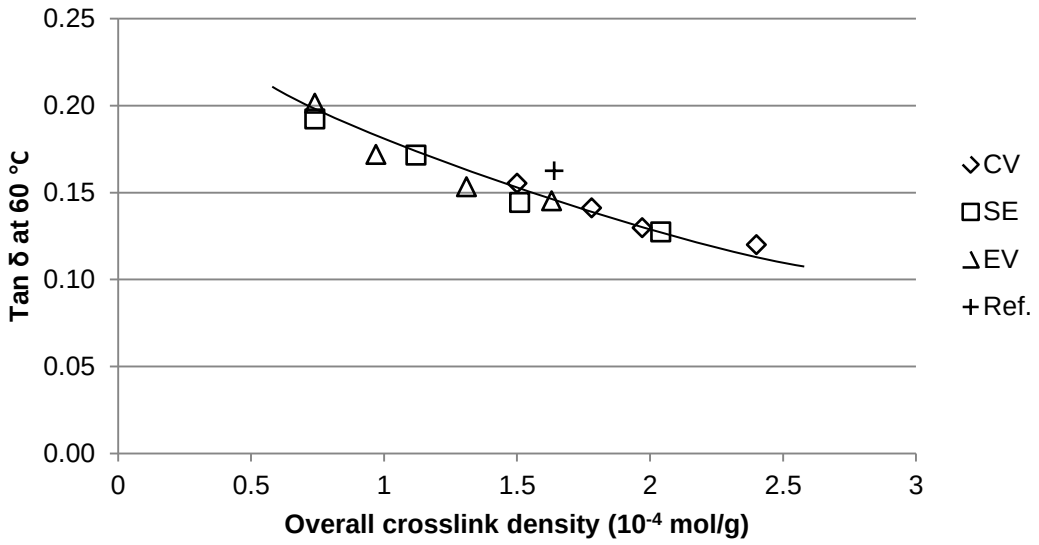

Figure 9: Tan δ at 60 °C values versus overall crosslink density.

Since the strain level at which the tan δ was measured is 6 %, it may be assumed that none of the existing crosslink types undergoes breaking or recombination as in the case of the measurements of the tensile strength and the storage modulus at 90 % strain. Therefore, the overall crosslink density is the only factor that differentiates the various compounds. The energy can be stored and released more efficiently and without a loss in a compound characterized by a higher overall crosslink density: an increased number of chemical nodes connecting the polymer chains decreases the possibility of their rearrangements, which results in a reduced energy dissipation.

Tan δ at low temperatures: known insufficient indicator of wet skid resistance

As shown in Figure 10, a rising amount of curatives in the compounds has an influence on the glass transition temperature (as is well known), but only a minor one on the height of the tan δ peak. Starting from approximately 10 °C onwards, the differences between the individual curves gradually rise. For each vulcanization system, the compounds with the highest loadings of

curatives are characterized by the lowest hysteresis at higher temperatures, as already seen in Figure 9.

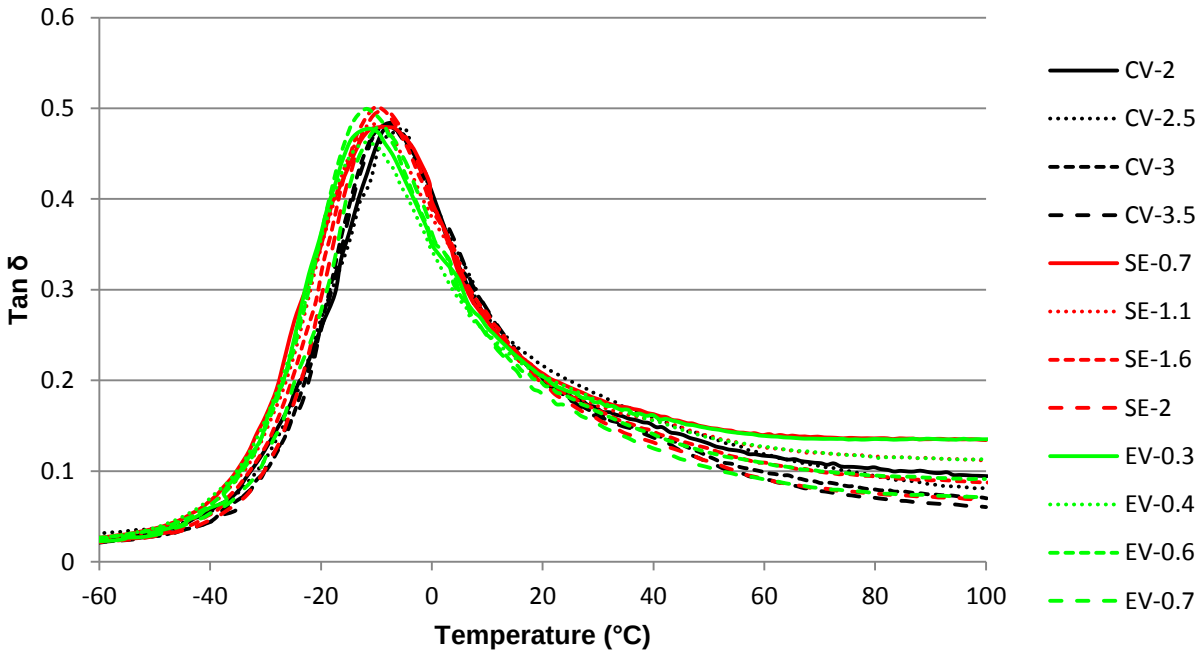

Figure 10: Tan δ values in temperature sweep mode for compounds with different vulcanization systems.

The increase in the overall crosslink density is large enough to cause significant changes in the segmental mobility of the elastomer chains which is visible in the increasing glass transition temperature, see Table 3. For the compound with the efficient vulcanization system, the average T_g is around -12 °C, followed by the compounds with the semi-efficient system, for which the T_g is equal to -9 °C, and the conventional system with the highest T_g of around -7 °C. Figure 12 demonstrates the influence of the sulfur / accelerator ratio on the glass transition temperature T_g. The higher the relative sulfur content the higher the T_g value. A higher sulfur content (knowing that this means in this experiment as well an increasing accelerator concentration for each

system) leads to a higher crosslinking density (see Fig. 12) which causes a stiffer network and therefore allows less possibilities of a free chain movement. As a result of this, T_g rises (Fig. 11).

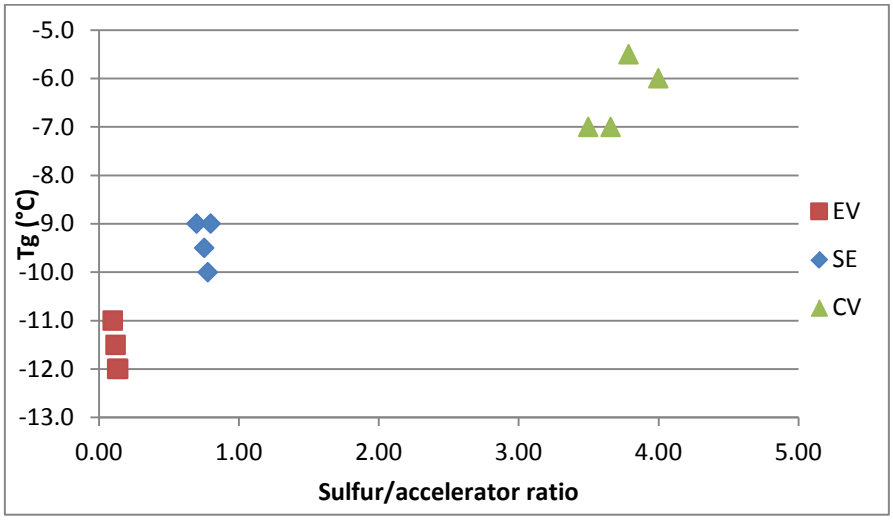

Figure 11: Glass transition temperature depending on the sulfur / accelerator ratio.

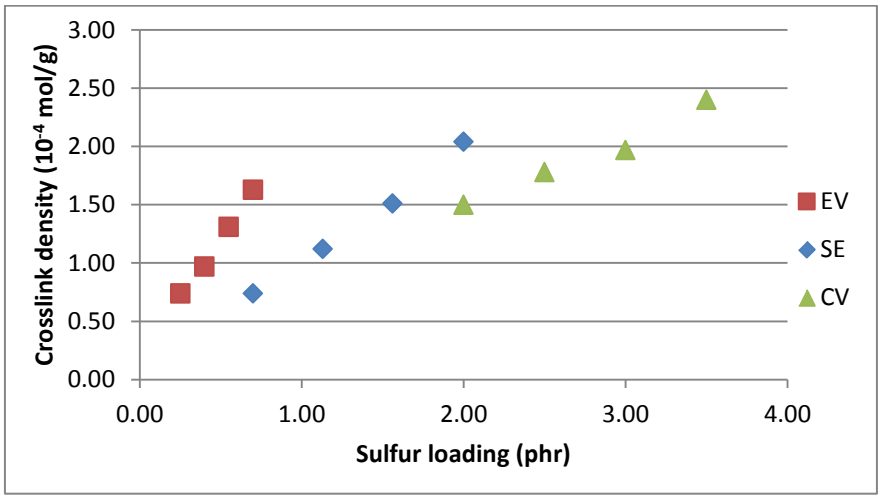

Figure 12: Crosslinking density depending on the sulfur loading.

Furthermore, a similar height of the tan δ maximum demonstrates that even substantial changes in the crosslink density cannot significantly change the hysteresis in the glass transition

temperature range, hence the amount of polymer chains which contribute to the intermolecular friction remains unaffected. Only a variation in the adsorption of the polymer chains at the filler surface which virtually lowers the fraction of the polymer which undergoes the glass transition can cause changes in the peak height. Change in the crosslinking system does not increase nor decrease the total amount of chains undergoing segmental, intermolecular friction. Hence the peak height remains unaffected.

Table 1: Comparison of dynamic properties at the glass transition temperature.

Sample code	x-link density 10^{-4} mol/g	Tg (°C)	G' (MPa)	G" (MPa)
CV-2	1,50	-6,0	115	53
CV-2.5	1,78	-5,5	97	39
CV-3	1,97	-7,0	100	48
CV-3.5	2,40	-7,0	89	43
SE-0.7	0,74	-9,0	101	48
SE-1.1	1,12	-9,5	95	46
SE-1.6	1,51	-10,0	94	47
SE-2	2,04	-9,0	100	50
EV-0.3	0,74	-11,0	88	42
EV-0.4	0,97	-11,5	88	41
EV-0.6	1,31	-12,0	99	49
EV-0.7	1,63	-12,0	87	43

At higher temperatures, above 10 °C, the decreasing hysteresis of compounds (Fig. 10) with an increasing loading of curatives is the result of the rising overall crosslink density. At temperatures above the glass transition, the polymer chains are more mobile and can perform quasi-liquid cooperative rearrangements, which is the cause of the energy dissipation. A higher overall crosslink density of the compounds reduces the possibility of these quasi-liquid cooperative rearrangements, what is visible in the lower hysteresis.

Side force coefficient: better predictor for wet skid resistance

The side force coefficient values obtained by LAT 100 measurements increase for each crosslinking system with increasing loading of curatives and overall crosslink density, see Figure 13. However, the differences in side force coefficient between the samples are small. The minimum and maximum values of the side force coefficient are very similar for all three curing systems.

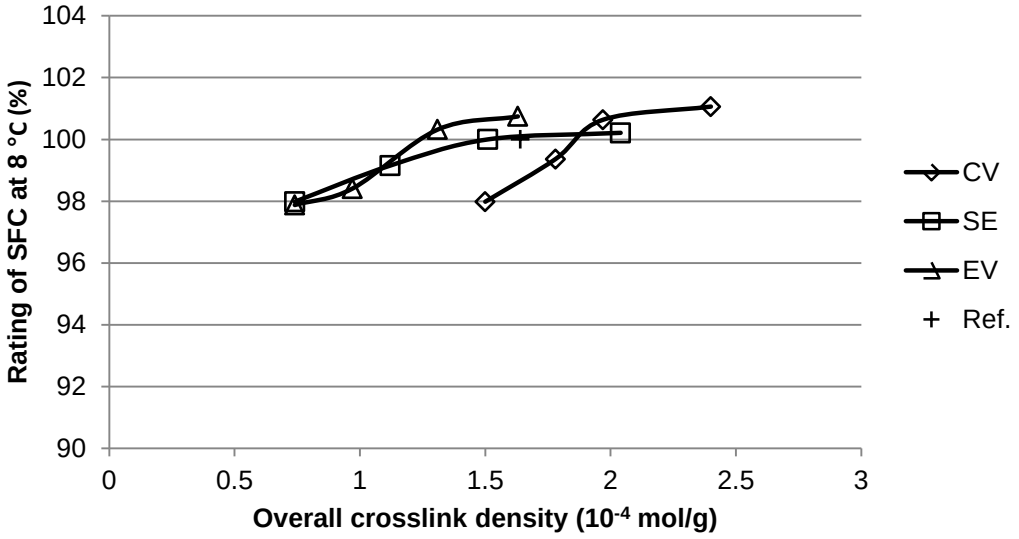

Figure 13: Side force coefficient rating at 8 °C versus overall crosslink density.

These minor differences in the side force coefficient of the samples can be explained when the dynamic properties at lower temperatures, from 0 to 20 °C are considered, see Figure 10. The different vulcanization systems all show similar values of the hysteresis at lower temperatures. The value of the storage modulus for all samples measured at the tan δ peak is in the range of 90 to 100 MPa. The differences in the measured stiffness are therefore too small to show an effect on the side force coefficient.

Another factor which could cause these small differences in SFC-ratings is the rising hardness of the compounds with increasing loading of the curatives. A comparison of the side force coefficient and Shore A hardness values is shown in Figure 14. The side force coefficient correlates with hardness for each vulcanization system separately. However, when for example the minimal values of the side force coefficient for the efficient and conventional systems are compared with each other, it is clear that in spite of a substantial hardness difference of 8 °ShA between the samples, the same value of the side force coefficient is registered. Therefore, a clear correlation between hardness and the side force coefficient does not exist as this study has shown: a correlation only exist within a series with the same type of curing system.

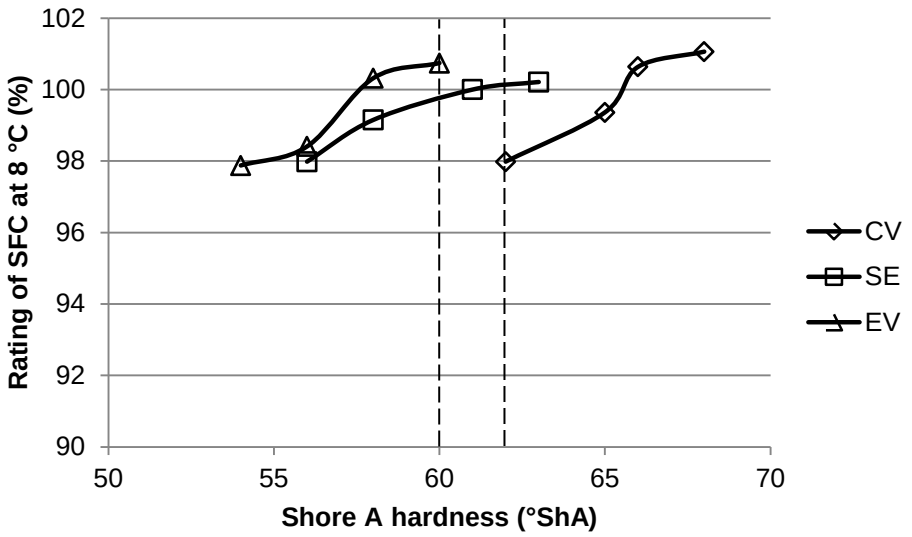

Figure 14: Rating of the side force coefficient versus Shore A hardness.

The data shown in Figure 13 also allow the comparison of the individual systems with a similar hardness. When the hardness in the range of 60 to 62 °ShA is considered, the efficient curing system is characterized by the highest value of the side force coefficient followed by the semi-efficient and conventional systems.

CONCLUSIONS

- A maximum in tensile strength is pronounced for the efficient curing system, and the least visible for the conventional vulcanization system. The samples with the efficient vulcanization are also characterized by the highest values of the tensile strength, which can be caused by the lower crack propagation ability of the material with lower overall crosslink density together with a higher bond energy of the mono- and disulfidic crosslinks.

- Increasing the overall crosslink density of the compounds causes a rise in the glass transition temperature by about 5 °C between the compounds with the efficient curing system and the conventional system. However, no major changes in the height of the tan δ peak are registered. Apparently, only variations in the polymer immobilization on the filler surface can lead to changes in the peak height, for instance in the case of silicas differing in the specific surface area or different coupling agents.
- The values of tan δ at 60 °C are decreasing with increasing overall crosslink density of the compounds. This trend is independent of the crosslink types, as at the strain level applied during the measurement the ability towards recombination of longer poly-sulfidic crosslinks is not yet playing a role.
- The compounds with the different curing systems are characterized by only a small changes in the LAT-100 side force coefficient. This could be caused by minor differences in the storage and loss moduli of the compounds at low temperatures. For a similar value of hardness the efficient and semi-efficient curing systems give slightly higher values of the SFC in comparison with a conventional system.

ACKNOWLEDGMENTS

This project was carried out in the framework of the innovation program ‘GO Gebundelde Innovatiekracht’, and funded by the ‘European Regional Development Fund’. The project partners Apollo Tyres Global R&D, Enschede, University of Twente (Tire-Road Consortium), Enschede, and Elastomer Research and Testing B.V., Deventer, all in the Netherlands, are gratefully acknowledged for their assistance.

REFERENCES

[1] J. Lal, Rubber Chem. Technol. 43 (1970) 664.
[2] C.G. Moore, B.R. Trego, J. Appl. Polym. Sci. 5 (1961) 299.
[3] C.M. Kok, V.H. Yee, Eur. Polym. J. 22 (1986) 341.
[4] M. Nasir, G.K. Teh, Eur. Polym. J. 24 (1988) 733.
[5] W. Salgueiro, A. Marzocca, A. Somoza, G. Consolati, S. Cerveny, F. Quasso, S. Goyanes, Polymer 45 (2004) 6037.
[6] A.J. Marzocca, S. Goyanes, J. Appl. Polym. Sci. 91 (2004) 2601.
[7] R. Joseph, K.E. George, D.J. Francis, J. Appl. Polym. Sci. 35 (1988) 1003.
[8] J.A. Brydson, “Rubber Chemistry”, Applied Science Publishers Ltd, London (1978) Ch. 8.
[9] L. Bateman, J.I. Cunneen, C.G. Moore, L. Mullins, "The chemistry and physics of rubber-like substances", John Wiley & Sons, New York (1963) 715.
[10] B.A. Dogadkin, Z.N. Tarasova, Rubber Chem. Technol. 27 (1954) 883.
[11] K.J. Saunders, “Organic Polymer Chemistry”, 2nd ed. Chapman & Hall, London, (1988) Ch. 20.
[12] W. Scheele, Rubber Chem. Technol. 34 (1961) 1306.
[13] B. Saville, A.A. Watson, Rubber Chem. Technol. 40 (1967) 100.
[14] M. Porter, “The Chemistry of Sulfides,” A.V. Tobolsky, Ed., John Wiley & Sons, Inc., New York (1968).
[15] M. Porter, “Organic Chemistry of Sulfur,” S. Oae, Ed., Plenum Press, New York (1977).
[16] J.D. Ferry, R.G. Mancke, E. Maekawa, Y. Oyanagi, R.A. Dickie, Rubber Chem. Technol. 39 (1966) 897.
[17] G.R. Hamed, N. Rattanasom, Rubber Chem. Technol. 75 (2002) 323.
[18] G.R. Hamed, N. Rattanasom, Rubber Chem. Technol. 75 (2002) 935.
[19] D.M. Bieliński, Archives of Civil and Mechanical Engineering, 7 (2007) 15.
[20] D.M. Bieliński, A. Stępkowska, Archives of Civil and Mechanical Engineering, 13 (2013) 192.
[21] J. Ramier, L. Chazeau, C. Gauthier, L. Guy, M.N. Bouchereau, Rubber Chem. Technol. 80 (2007) 183.
[22] H.W. Greensmith, L. Mullins, A.G. Thomas, “The Chemistry and Physics of Rubber-like substances”, Applied Science Publishers Ltd, London (1963) Ch. 10.
[23] L. Mullins, “Relation between structure and properties”, Proc. NRPRA Jubilee Conf. Cambridge (1964).
[24] Coran, A. Y. In Science and Technology of Rubber, 2nd ed.; Mark, J. E.; Erman, B.; Eirich, F. R., Eds.; Academic Press: New York, (1994).
[25] A.H.M Schotman, R.N. Datta, Rubber Chem. Technol. 69 (1996) 727.
[26] B. Ellis, G.N. Welding, Rubber Chem. Technol. 37 (1964) 571.
[27] C.G. Moore, J. Polym. Sci. 32 (1958) 503.
[28] L. Gonzalez, A. Rodriguez, J.L. Valentin, A. Marcos-Fernandez, P. Posadas, Kautschuk Gummi Kunststoffe, 58 (2005) 638.
[29] M. Heinz, K.A. Grosch, 167th Technical meeting of the Rubber Division ACS, May 16 -18 2005, San Antonio, Texas, USA